Please cite this article in press as: Gao et al., Specific Kinematics and Motor-Related Neurons for Aversive Chemotaxis in *Drosophila*, Current Biology (2013), http://dx.doi.org/10.1016/j.cub.2013.05.008

Current Biology *23*, 1–10, July 8, 2013 ©2013 Elsevier Ltd All rights reserved http://dx.doi.org/10.1016/j.cub.2013.05.008

Article

# Specific Kinematics and Motor-Related Neurons for Aversive Chemotaxis in *Drosophila*

**Xiaojing J. Gao,[1] Christopher J. Potter,[1,3] Daryl M. Gohl,[2] Marion Silies,[2] Alexander Y. Katsov,[2,4] Thomas R. Clandinin,[2,*] and Liqun Luo[1,*]**

[1]Howard Hughes Medical Institute and Department of Biology
[2]Department of Neurobiology
Stanford University, Stanford, CA 94305, USA

## Summary

**Background:** Chemotaxis, the ability to direct movements according to chemical cues in the environment, is important for the survival of most organisms. The vinegar fly, *Drosophila melanogaster*, displays robust olfactory aversion and attraction, but how these behaviors are executed via changes in locomotion remains poorly understood. In particular, it is not clear whether aversion and attraction bidirectionally modulate a shared circuit or recruit distinct circuits for execution.

**Results:** Using a quantitative behavioral assay, we determined that both aversive and attractive odorants modulate the initiation and direction of turns but display distinct kinematics. Using genetic tools to perturb these behaviors, we identified specific populations of neurons required for aversion, but not for attraction. Inactivation of these populations of cells affected the completion of aversive turns, but not their initiation. Optogenetic activation of the same populations of cells triggered a locomotion pattern resembling aversive turns. Perturbations in both the ellipsoid body and the ventral nerve cord, two regions involved in motor control, resulted in defects in aversion.

**Conclusions:** Aversive chemotaxis in vinegar flies triggers ethologically appropriate kinematics distinct from those of attractive chemotaxis and requires specific motor-related neurons.

## Introduction

All motile organisms are guided by environmental chemical cues. *Escherichia coli* aggregates at an attractant source by coupling the frequency of random changes in orientation to changes in attractant concentration over time [1]. *Caenorhabditis elegans* uses an analogous mechanism but biases the reorientation events according to the direction of the gradient [2]. Still more sophisticated mechanisms, involving active sampling, specific orienting movements, and decision making, underlie chemotactic strategies in *Drosophila* and mammals [3–6]. These strategies rely on complex neural processing, but the circuits for their execution remain unknown.

Adult *Drosophila* represents an outstanding model for investigating the neural control of chemotaxis. Flies are similar to vertebrates in the organization of their olfactory circuits [7]; their bipartite central nervous systems, comprising a brain and a ventral nerve cord (VNC)/spinal cord; and their complex repertoire of movements, made possible by articulated appendages. As a result, olfactory-motor transformations in flies are likely distinct from those in simpler organisms. Flies seek odorants indicative of food [8–11] and avoid many volatile chemicals, especially at high concentrations [10–13]. Their olfactory behavior has been used extensively to study olfactory coding [3, 8–10] and neural plasticity [14]. However, beyond the circuits for sensing and processing olfactory information, the neurons that execute these behaviors are largely unknown. The genetic tools in *Drosophila* enable access to specific neural components [15]. Furthermore, recent advances in the tracking of freely walking flies make it possible to screen for behavioral defects and allow dissection of the temporal details of chemotactic behavior [16, 17].

Chemotactic behaviors can be elicited by dedicated olfactory receptor neurons [12, 13]. Moreover, distinct input channels were reported to mediate aversion and attraction to vinegar at different concentrations [8]. To what extent is this sensory separation preserved as information flows through the nervous system? One possibility is that attraction and aversion converge onto one circuit that is bidirectionally regulated; alternatively, these opposing tasks may each recruit distinct circuits for execution. Here we combine quantitative analysis of behavior with genetic perturbations to compare aversive and attractive chemotaxes. Our results demonstrate that these tasks are characterized by distinct kinematics and that aversion engages specific neuronal populations for execution.

## Results

### Aversion and Attraction Both Enrich Turns, but the Kinematics Differ

To observe adult fly chemotaxis with high temporal resolution and throughput, we simultaneously tested 15–20 flies in a four-quadrant arena [8], recording the trajectories of each individual [16]. A typical experiment began with 2.5 min of air delivery to all four quadrants ("control period") and continued for 5 min more after an odorant entered one quadrant ("odorant period"). As previously reported, control flies were robustly repelled by 10% acetic acid (Figure 1A), as well as a number of other compounds at high concentration (see Figure S1 available online; data not shown), and were attracted to apple cider vinegar (Figure 1B).

A variety of changes in the movements of individual flies might account for the changes in their spatial distribution during chemotaxis. Visual inspection suggested that flies approaching the aversive quadrant from an air quadrant turned back near the quadrant boundary, a behavior that could directly contribute to aversion (Figures 1D and S1; Movie S1). Conversely, turns toward an attractive odorant source were also observed, although at a lower frequency (Figure 1E; Movie S2). To describe turns under both aversive and attractive conditions, we approximated the contour lines of odorant concentrations by concentric circles centered on the bottom

[3]Present address: The Solomon H. Snyder Department of Neuroscience, The Johns Hopkins University School of Medicine, Baltimore, MD 21205, USA
[4]Present address: Laboratory of Neural Circuits and Behavior, The Rockefeller University, New York, NY 10065, USA
*Correspondence: trc@stanford.edu (T.R.C.), lluo@stanford.edu (L.L.)

Please cite this article in press as: Gao et al., Specific Kinematics and Motor-Related Neurons for Aversive Chemotaxis in *Drosophila*, Current Biology (2013), http://dx.doi.org/10.1016/j.cub.2013.05.008



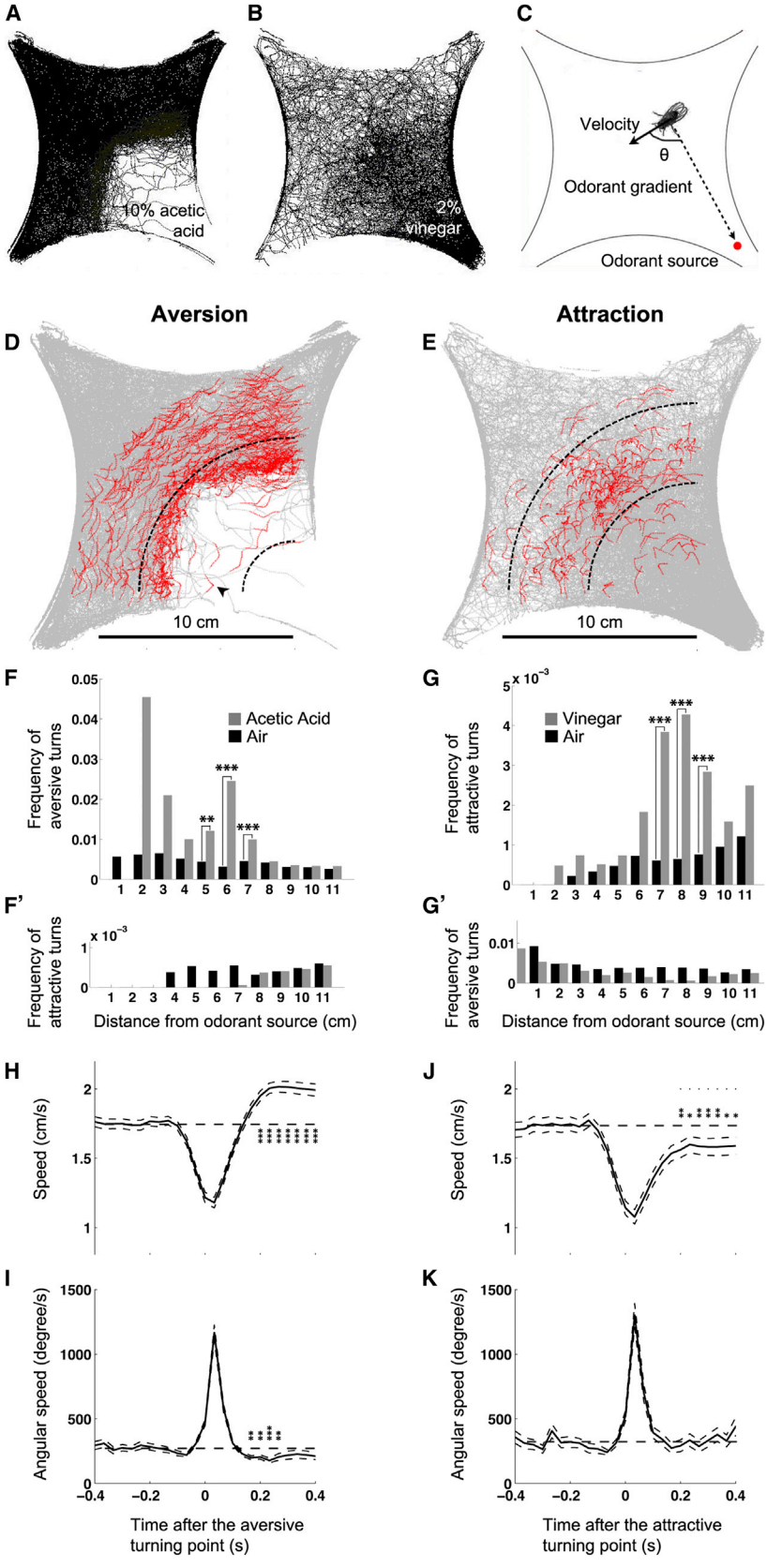


Figure 1. Aversive and Attractive Chemotaxes Enrich Turns but Differ in Their Kinematics

(A and B) Trajectories of *UAS-shi$^{ts1}$*/+ flies with 10% acetic acid (A) or 2% vinegar (B) in the bottom right quadrant. Each black dot represents the appearance of one fly in one frame, and data were pooled over all periods, as specified in Figure S3.

(C) Definition of the orientation angle θ. Red dot represents the odorant source. Dashed arrow represents the approximated direction of the odorant gradient. Solid arrow represents the direction of the velocity.

(D and E) Turn segments (red) flanking the aversive turning points in response to 10% acetic acid (D) or attractive turning points in response to 2% vinegar (E). Arrowhead in (D) represents an exemplary turning point. Gray dots are the same as black dots in Figures 1A and 1B. The dashed lines specify the borders (2.5–7.5 cm in D and 5.5–9.5 cm in E) of areas for data collection in Figures 1H–1K.

(F–G′) The relation between the distance from the odorant source and the frequency of aversive (F and G′) or attractive (F′ and G) turns in chemotactic aversion (F and F′) and attraction (G and G′). Compared to the air control, the aversive odorant (acetic acid) condition enriches aversive turning points (F), whereas the attractive odorant (vinegar) condition enriches attractive turning points (G). For each bin, the number of aversive turns against the total number of tracked fly positions between the control and the odorant periods were compared with a chi-square test, and only significantly different bins were indicated.

(H–K) The temporal profiles of speed (H and J) and angular speed (I and K) around the aversive (H and I) or attractive (J and K) turning points. Solid traces represent the means of all individual data points over time; dashed traces represent mean ± SEM. The comparisons were made between mean speed or angular speed before turning (–0.4 s to –0.2 s) and at every time point after turning (0.17 s to 0.4 s), with the turning point as time 0. Only significantly different time points were indicated. (Wilcoxon test; n = 387 for aversion, n = 203 for attraction).

Throughout the paper: *p < 0.05, **p < 0.01, ***p < 0.001.

right corner of the arena ("odorant source," red dot in Figure 1C), based on direct visualization of airflow in the arena (Movie S3). By definition, the odorant gradient at any position points from that position to the odorant source (Figure 1C). We define the "aversive turning point" of a trajectory as the point closest to the odorant source (arrowhead in Figure 1D denotes one example), and the short segment of trajectory flanking the turning point is defined as an "aversive turn" (red segments in Figure 1D). Similarly, the "attractive turning point" of a trajectory was defined as the point farthest away from the odorant source, marking the corresponding trajectory segment as an "attractive turn" (red segments in Figure 1E). We examined how often such turns occurred at different distances from the odorant source, normalized by the total number of data points at the same distance. For both aversion and attraction, the corresponding turns were enriched within certain ranges (Figures 1F, 1G, and S1). As expected, attractive turns were not enriched in aversion (Figures 1F′ and S1), and aversive turns were not enriched in attraction (Figure 1G′).

Please cite this article in press as: Gao et al., Specific Kinematics and Motor-Related Neurons for Aversive Chemotaxis in *Drosophila*, Current Biology (2013), http://dx.doi.org/10.1016/j.cub.2013.05.008



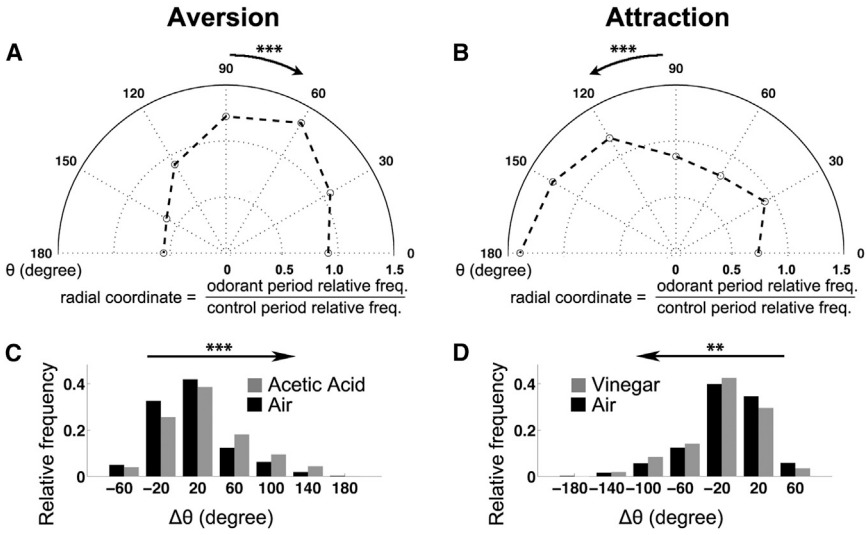


Figure 2. Odorant Gradients Modulate Turn Initiation and Direction

(A and B) Distribution of velocity orientations in the border area (see Figures 1D and 1E) upon turn initiation in aversion (A; n = 2,954 for the control period, n = 2,276 for the odorant period) or attraction (B; n = 4,642 for the control period, n = 4,238 for the odorant period) in the polar coordinate system. Radial coordinate represents the ratio of the relative frequency during the odorant period and the relative frequency during the control period. Angular coordinate represents θ (defined in Figure 1C; in degrees) upon turn initiation. The velocity orientation upon turn initiation is biased toward the odorant source in aversion (arrow pointing to the right in A) and away from the odorant source in attraction (arrow pointing to the left in B) compared to their control periods, respectively.

(C) Distribution of Δθ after turning, for events initiated when the flies were moving toward the odorant source (red dot in Figure 1C) during the control (n = 1,368) and aversive (n = 1,322) odorant period. The arrow pointing to the right indicates that the whole distribution during the aversive period is biased to align the flies against the odorant gradient (>0°).

(D) Distribution of Δθ after turning, for events initiated when the flies were moving away from the odorant source (red dot in Figure 1C) during the control (n = 1,887) and attractive (n = 2,081) odorant period. The arrow pointing to the left indicates that the whole distribution during the attractive period is biased to align the flies with the odorant gradient (>0°).

All statistical significance in this figure was assessed by Wilcoxon test. The comparisons were made between the entire distributions of θ in the control period and the odorant period in (A) and (B) and the entire distributions of Δθ in the control period and the odorant period in (C) and (D). The genotype is *UAS-shi$^{ts1}$/+*, which also serves as a control for Figure 4.

To determine whether these turns represented quantitatively similar changes in behavior, we examined the fine structure of turning movements, based on the region where turns were enriched (between the dashed curves in Figures 1D, 1E, and S1). We calculated the average walking speed and angular speed of aversive and attractive turns aligned by the "turning points" (as defined above). As expected, turns were associated with a reduction in speed (Figures 1H, 1J, and S1) and a peak in angular speed (Figures 1I, 1K, and S1), the magnitudes and durations of which were almost identical between aversion and attraction. However, after aversive turns, speed increased significantly (Figures 1H and S1), and angular speed decreased significantly (Figures 1I and S1) compared to the baseline values before turns. Thus, after aversive turns, flies moved more quickly and followed straighter paths. Neither of these modulations was observed in attractive turns, and the speed after a turn even decreased (Figures 1J and 1K). The difference between aversive and attractive turning kinematics was not simply due to the asymmetric geometry in our definition of turning points (see Experimental Procedures), because aversive turns during the control period lacked the speed increase and angular speed decrease observed in aversive turns during the odorant period (Figure S1, compare to Figures 1H and 1I). Intriguingly, these odorant-free turns were qualitatively similar to attractive turns, implying that attraction, unlike aversion, might not induce specific types of turns. Finally, we note that, despite our selection of a region of interest, none of these conclusions were sensitive to the precise borders chosen, because those chosen included 45% of aversive turns (red segments in Figure 1D) and 64% of attractive turns (red segments in Figure 1E). As a result, adding or removing a few turn segments by shifting the borders did not significantly alter the ensemble statistics. Thus, both aversion and attraction increase the frequency of turning events as flies transition into or out of the odorant quadrant, respectively, but these turns are quantitatively different, suggesting different underlying executive programs.

## Odorants Modulate Turn Initiation and Direction

We envisioned two mechanisms that could contribute to the enrichment of aversive turns in aversion (or attractive turns in attraction). First, a fly could modulate the frequency of turn initiation depending on whether it is moving up or down an odorant gradient. Second, when a fly was turning, it could utilize the spatial odorant gradient to determine its turn direction. We tested whether either or both of these two mechanisms were used.

To test for modulation of the frequency of turn initiation, we identified all turns (see Experimental Procedures) and classified them by the direction of fly movement prior to turn initiation. To determine the direction of movement, we calculated the angle θ between each fly's velocity and the odorant gradient ($0° \leq \theta \leq 180°$, Figure 1C). When $\theta = 0°$, the fly was walking exactly toward the odorant source; at $\theta = 180°$, the fly was moving exactly in the opposite direction. We found that, in the aversion assay, flies were more likely to be moving toward the odorant source (up the gradient) right before turns began ($\theta < 90°$, Figures 2A and S2), while in the attraction assay, flies were more likely to be moving away from the source ($\theta > 90°$, Figure 2B). Odorant concentration changes thus modulate the frequency of turn initiation in both attractive and aversive contexts.

We next tested whether the direction of induced turns were influenced by the direction of the odorant gradient. We generated the metric Δθ by subtracting the absolute value of θ at turn initiation from that at turn termination. A positive or negative Δθ means that the turn shifts the walking direction away from or toward the odorant source, respectively. For turns initiated when the flies were moving toward the aversive odorant source, we compared the Δθ distribution to that observed in

Please cite this article in press as: Gao et al., Specific Kinematics and Motor-Related Neurons for Aversive Chemotaxis in *Drosophila*, Current Biology (2013), http://dx.doi.org/10.1016/j.cub.2013.05.008



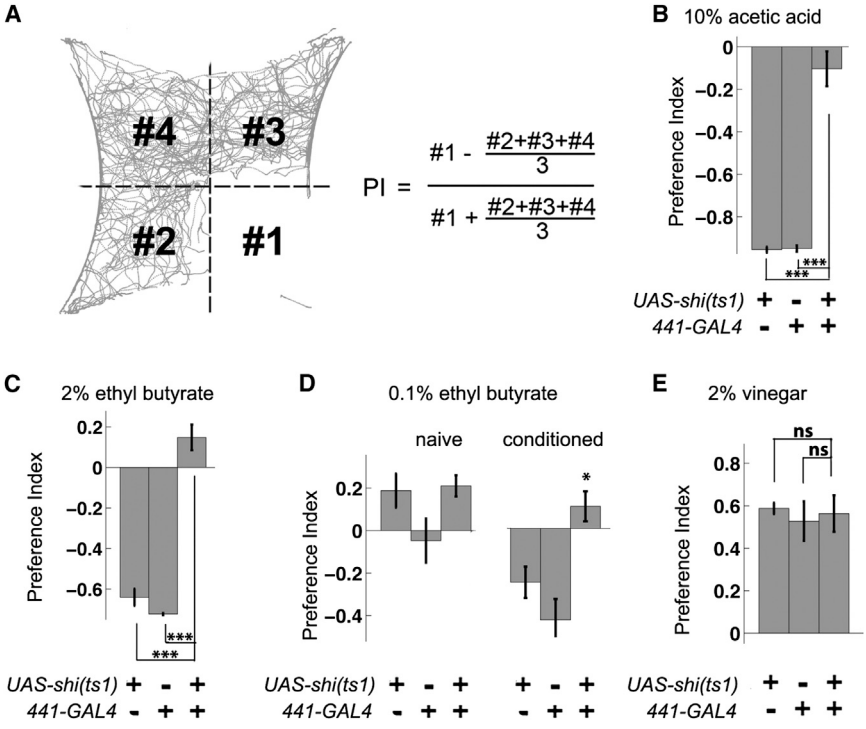


Figure 3. *441* > *shi$^{ts1}$* Affects Aversive, but Not Attractive, Chemotaxis

(A) Definition of the preference index (PI). Each number represents all positions flies visit in a particular quadrant counted over a defined period of time. For aversion, the PI was calculated 2.5–5 min after the odorant onset, when the index reached a steady state (Figure S3). For attraction, the PI was calculated 1–3 min after the odorant onset to reduce the impact of habituation (Figure S3).

(B) Strong aversion to 10% acetic acid in control animals is almost completely abolished in *441* > *shi$^{ts1}$* flies.

(C) *441* > *shi$^{ts1}$* abolishes aversion to 2% ethyl butyrate.

(D) *441* > *shi$^{ts1}$* abolishes learned aversion. To associate the naturally attractive or neutral odorant (0.1% ethyl butyrate) with a negative valence, we repetitively delivered it to the flies coupled with electric shocks right before testing in the arena.

(E) *441* > *shi$^{ts1}$* does not affect the PI to 2% vinegar. Columns are for mean PIs of multiple independent runs; error bars represent SEM ($n \geq 4$). (B), (C), and (E): t test was performed with Holm-Bonferroni post hoc correction; (D): two-way ANOVA tests the significance of the interaction between genotype and conditioning.

the control period of the same experiment. Given that we selected the turns whose initial $\theta$ was smaller than 90°, the $\Delta\theta$ distribution was inherently biased to be above 0°. However, the frequency of positive $\Delta\theta$ was further increased under the aversive condition compared with controls, demonstrating that the local odorant gradient indeed modulated the flies' turn direction (Figures 2C and S2). An attractive odorant gradient modulated turn direction in a similar fashion, enriching negative $\Delta\theta$ in turns triggered while moving down the gradient (Figure 2D). Thus, odorant gradients modulate the direction of turning in both aversion and attraction.

In summary, turns evoked during chemotaxis involve both mechanisms proposed at the beginning of this section. When a fly walks toward an aversive odorant (or away from an attractive odorant), it is more likely to start turning, and the turn direction is biased away from the aversive odorant (or toward the attractive odorant).

## A Screen for Neurons Necessary for Aversion

Aversion and attraction could reflect different dynamical states of the same motor control circuit or could engage distinct circuits for execution. To distinguish between these possibilities, we manipulated the underlying circuits. Under our experimental conditions, aversion was robust while attraction was sensitive to genetic background. We therefore screened for neurons necessary for aversion to 10% acetic acid. We chose 103 *GAL4* lines from an integrase swappable in vivo targeting element enhancer trap collection [18], each of which allows transgene expression in specific neuronal populations. These lines were selected for relatively sparse expression and against expression in olfactory receptor neurons or projection neurons. To impair synaptic output from targeted neurons, we expressed *UAS-shibire$^{ts1}$* (*UAS-shi$^{ts1}$*), which acutely abolishes synaptic transmission at the restrictive temperature used in our assays [19].

The metrics described above were data intensive and might not capture every aspect of chemotaxis, making them impractical for a screen. We therefore defined a preference index (PI) as a comprehensive chemotaxis indicator (Figure 3A). A PI of 1 means that the flies always remain within the odorant quadrant, a PI of 0 means that they spend as much time in the odorant quadrant as in the air quadrants, and a PI of –1 means that they never enter the odorant quadrant. We identified four lines that strongly impaired aversion (Figure S3) and characterized in detail two of these, *441-GAL4* and *918-GAL4*.

## *441*-Targeted Silencing Affects Aversion, but Not Attraction

Expression of *UAS-shi$^{ts1}$* under the control of *441-GAL4* (*441* > *shi$^{ts1}$*) almost completely abolished aversion to 10% acetic acid, as measured with the PI (Figure 3B). This line therefore allowed us to address whether the circuit elements necessary for acetic acid aversion are shared by other chemotactic behaviors. We found that *441* > *shi$^{ts1}$* flies also abolished aversive responses to both 2% ethyl butyrate (Figure 3C) and 0.1% E2-hexenal (Figure S3). Flies can also be conditioned to avoid naturally attractive or neutral odorants through their association with electric shocks. Despite its distinct origin from innate aversion, learned aversion to 0.1% ethyl butyrate was also abolished by *441* > *shi$^{ts1}$* expression (Figure 3D). *441+* cells are thus broadly required for olfactory aversion. Interestingly, the attractive response to vinegar odor as measured by PI was completely unaffected (Figure 3E). These results implied a separation of neural circuits for olfactory aversion and attraction.

## *441-GAL4+* Cells Regulate the Completion of Aversive Turning

We next examined the possible behavioral mechanisms underlying the abolition of aversion in *441* > *shi$^{ts1}$* flies using

Please cite this article in press as: Gao et al., Specific Kinematics and Motor-Related Neurons for Aversive Chemotaxis in *Drosophila*, Current Biology (2013), http://dx.doi.org/10.1016/j.cub.2013.05.008



our kinematic metrics. Unlike control flies, which increased aversive turns in response to 10% acetic acid (Figures 1F and 4B), *441* > *shi$^{ts1}$* flies did not (Figure 4A). To understand how *441* > *shi$^{ts1}$* disrupts aversive turns, we analyzed turn initiation and direction. Intriguingly, while *441* > *shi$^{ts1}$* flies were still biased to initiate turning when moving toward the aversive odorant source, just as in controls (Figure 4C, compare with Figures 2A and 4D), they lost all directional modulation of $\Delta\theta$ (Figure 4E, compare to Figures 2C and 4F). *441* > *shi$^{ts1}$* flies thus still sensed the aversive odorant and initiated turns but failed to complete the late stages of the turning pattern necessary to appropriately reorient themselves.

If *441-GAL4* labeled circuit components necessary for the execution of an aversion-specific motor program, artificial activation of these cells might trigger elements of this program. To test this, we expressed Channelrhodopsin2 with *441-GAL4* (*441* > *ChR2*), allowing *441+* neurons to be activated by light [20], while incorporating a *norpA* mutation to block phototransduction. In these blind flies, angular speed peaked during blue light illumination (mimicking turning) and then dropped below baseline levels (mimicking turn suppression; Figure 4G, compare to Figure 4H). Moreover, this turn suppression coincided with a speed increase (Figure 4I, compare to Figure 4J). These kinematic changes are strikingly similar to those accompanying natural aversive turns (Figures 1H and 1I). Both resting and walking *441* > *ChR2* flies transitioned into fast walking after illumination (data not shown), indicating that the artificially induced locomotion overrode the flies' endogenous locomotion status. We note, however, that the light-induced pattern of neuronal activity was unlikely to completely mimic the natural pattern due to its synchrony and uniformity, which might account for the lack of an initial speed decrease during illumination. Alternatively, since *441+* circuits are not necessary for turn initiation (Figures 4C and 4D), it is possible that the speed decrease at the beginning of turns is controlled by neurons upstream of those labeled by *441-GAL4*. Thus, *441-GAL4* targets circuit components that are not only necessary for completion of aversive turns but also sufficient to induce aspects of kinematics characteristic of aversive turns.

The spatial distribution of *441* > *shi$^{ts1}$* flies in attraction appeared normal (Figure S4; also compare to Figure 1B), although the attractive turns were no longer enriched (Figure S4; also compare to Figure 1G) and the bias of turn initiation was changed (Figure S4; also compare to Figure 2B). Thus, aversion and attraction display both different turn kinematics and distinct dependence on turning. We infer that odorants may generate attraction through another mechanism.

### *441-GAL4* Targets Motor-Related Neural Structures

We sought to identify the *441+* cells responsible for aversion using intersectional strategies. *441-GAL4* labels glia and neurons in both the brain and the VNC (Figures 5A and 5A′). We first tested whether neuronal expression of *shi$^{ts1}$* was sufficient to cause the phenotype with a split GAL4 strategy [21]. We replaced the *GAL4* in *441-GAL4* with the *VP16* activation domain (AD) and introduced a second transgene expressing the *GAL4* DNA-binding domain (DBD) with a pan-neuronal promoter, *elav*. A functional *GAL4* was therefore only reconstituted in *441+elav+* cells when we combined *441-VP16AD* and *elav-GAL4DBD* to express *shi$^{ts1}$*. This manipulation still abolished aversion (Figure S5), indicating that neuronal expression of *shi$^{ts1}$* in *441+* cells is responsible for the aversion deficit. To assess the contributions of *441-GAL4* expressions in the brain versus the VNC, we introduced a VNC-specific suppressor of *GAL4*, *tsh-GAL80* [22]. *tsh-GAL80* greatly reduced *441-GAL4* expressions in both neurons and glia in the VNC, but not in the brain (Figures 5B and 5B′). In behavioral experiments, adding *tsh-GAL80* to *441* > *shi$^{ts1}$* flies restored the PI to about half of the PI observed in controls (Figure 5C), indicating that *441+tsh+* neurons were necessary for aversion. These data also suggest either that *tsh-GAL80* was not strong enough to completely block *441-GAL4* or that additional *441+tsh−* neurons contribute to aversion.

In the brain, *441-GAL4* has prominent expression in the ellipsoid body (EB, arrowhead in Figure 5A), which was reported to be necessary for olfactory aversion in a different assay [23]. To examine the role of these neurons, we generated two *EB-GAL80s* using enhancer fragments from a large collection of enhancer-*GAL4* fusions [24, 25] (Figure S5; data not shown). *R13C06-GAL80* effectively blocked *441-GAL4* in the EB (Figure 5D, open arrowhead) and partially restored aversion in *441* > *shi$^{ts1}$* flies (Figure 5C). Similar results were obtained using an independent *EB-GAL80* driven by a second enhancer, *R11F03* (Figure 5C). These data indicate that inactivation of EB neurons also contributed to loss of aversion when all *441+* neurons were inactivated. However, *EB-GAL4s* with the same two enhancers did not affect aversion when expressing *shi$^{ts1}$* (Figure S5), suggesting that *441+* EB neurons mediate aversive chemotaxis redundantly with other *441+* neurons. Finally, *R13C06-GAL80* and *tsh-GAL80* together did not restore the PI beyond the level of single *GAL80* (Figure 5C). This could be due to incomplete suppression of *441-GAL4* in the EB or *tsh+* neurons by GAL80; alternatively, *441* > *shi$^{ts1}$* may disrupt a third aversion-related circuit not accounted for by either *GAL80* line.

Given the implied importance of *441+* VNC neurons, we directly tested their sufficiency to induce locomotion in decapitated *441* > *ChR2* flies [26]. Headless *441* > *ChR2* flies immediately started to swing their legs upon illumination (Figure S5; Movie S4), a behavioral change that was never observed in controls lacking *441-GAL4* (Figure S5; Movie S5) or with a *GAL4* labeling many motor neurons (data not shown). Doubling the intensity of light stimulation caused nearly half of the headless flies to transition from leg swinging to nondirectional displacements, jumps, or forward walking (Figure S5; Movie S6). Although these headless flies did not maintain steady walking, perhaps due to the absence of brain-mediated coordination, this result demonstrated that activation of *441+* VNC neurons generated new locomotor patterns, even in sluggish, headless flies, reminiscent of the transition from resting to fast walking in intact flies.

We also attempted to narrow down the most likely VNC neurons involved in aversion using morphological analysis. *441* > *mCD8-GFP* only weakly labeled neuronal processes, and detailed studies of these neurons were confounded by glial labeling. We therefore expressed a strong dendritic marker (*DenMark*) with *441-GAL4* and removed glia expression using *repo-GAL80*. To facilitate comparison between individual VNCs, we took multiple image stacks under the same conditions both with and without *tsh-GAL80*, registered them to a standard VNC [27], and averaged the expression intensity of *DenMark* within each genotype (Figures 5E$_1$–5F$_2$′ and S5). *tsh-GAL80* suppressed *441* > *DenMark* expression in the abdominal ganglia (dashed boxes in Figures 5E$_1$–5E$_2$′; compare to Figures 5F$_1$–5F$_2$′), a region of the VNC that does not control locomotion. Outside the abdominal ganglia,

Please cite this article in press as: Gao et al., Specific Kinematics and Motor-Related Neurons for Aversive Chemotaxis in *Drosophila*, Current Biology (2013), http://dx.doi.org/10.1016/j.cub.2013.05.008



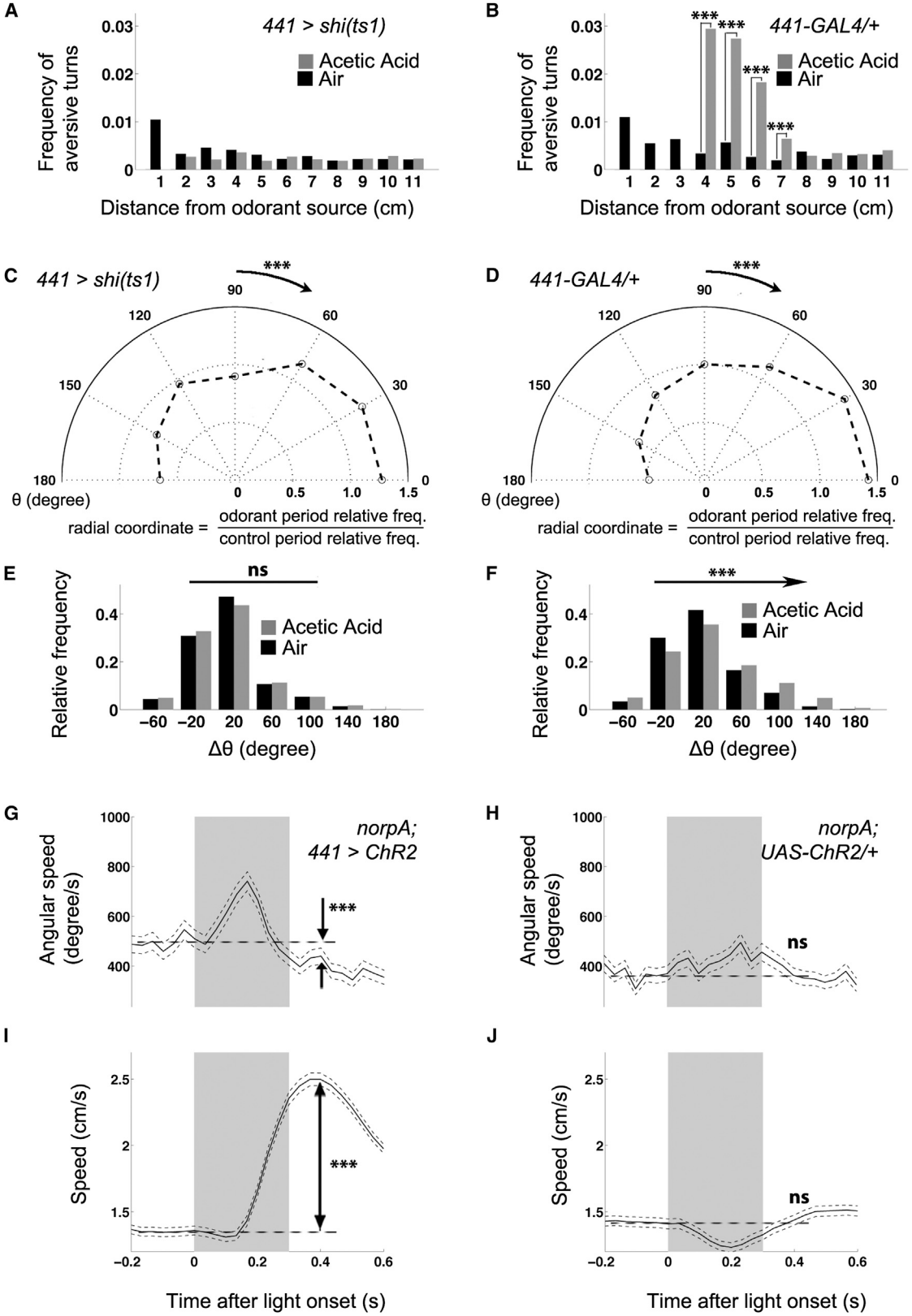


Figure 4. *441-GAL4* Defines Neurons for the Completion of Aversive Turns

(A and B) The enrichment of aversive turns in response to 10% acetic acid is abolished in *441 > shi$^{ts1}$* (A) compared to *441-GAL4* (B) and *UAS-shi$^{ts1}$/+* (Figure 1F) controls.

(C and D) The modulation of turn initiation, as measured by the distribution of θ upon turn initiation in the border area, still persists in *441 > shi$^{ts1}$* (C; n = 2,765 for the control period, n = 3,341 for the odorant period) compared to *441-GAL4/+* (D; n = 2,552 for the control period, n = 1,897 for the odorant period) and *UAS-shi$^{ts1}$/+* (Figure 2A) controls.

*(legend continued on next page)*

*441* > *DenMark* expression was only suppressed by *tsh-GAL80* in neurites extending from ventromedial cell bodies (arrows in Figures 5E$_1$, 5E$_2$, and S5; compare to the dashed arrows in Figures 5F$_1$ and 5F$_2$) to beneath the dorsal surface of the VNC (arrows in Figures 5E$_1'$ and 5E$_2'$; compare to the dashed arrows in Figures 5F$_1'$ and 5F$_2'$) and those along the midline within the VNC (arrowheads in Figures 5E$_1'$, 5E$_2'$, and S5; compare to the open arrowhead in Figures 5F$_1'$ and 5F$_2'$).

In summary, we identified two circuit element candidates, the EB and small subsets of VNC neurons, that are causally linked to aversive chemotaxis and are likely involved in motor control (see Discussion).

### *918-GAL4+* Neurons Are Also Required for Aversion and Overlap with *441+* VNC Neurons

The second line identified in our genetic screen (Figure S3), *918-GAL4*, strongly supported the importance of the VNC neural elements defined by *441-GAL4* for aversion. *918* > *shi$^{ts1}$*, like *441* > *shi$^{ts1}$*, attenuated aversion, but not attraction (Figures 6A–6C), a deficit that was fully rescued by *tsh-GAL80* (Figure 6A). *918-GAL4* appeared to label the *441+* ventromedial neurons as well, based on the stereotypic locations of their cell bodies (arrows in Figure 6D; compare to those in Figures 5E$_1$–5E$_1'$). Labeling of these ventromedial neurons was also suppressed by *tsh-GAL80* (Figure 6E, dashed arrows). In the brain, *tsh-GAL80* only suppressed *918* expression in some local interneurons in the antennal lobes (Figure S6).

To test whether *918-GAL4* and *441-GAL4* label the same VNC neurons and, if so, whether these neurons play essential roles in aversion, we replaced the *GAL4* in *441-GAL4* with *GAL80* at exactly the same genomic locus [18]. Indeed, *441-GAL80* rescued the aversion deficit in *918* > *shi$^{ts1}$* flies (Figure 6A). We used *UAS-mCD8-GFP* to visualize the pattern of *918-GAL4* after *441-GAL80* suppression but did not find any apparent effect (data not shown). We reasoned that the intersectional effect might be sufficient to alter behavior but insufficient to cause a change of expression visualized using a stable marker like m*CD8-GFP*. To sensitize our expression analysis, we utilized *UAS-CL1-GFP*, an unstable *GFP* with a degradation tag. The ventromedial cell bodies were labeled in *918* > *CL1-GFP* VNCs (Figure 6F, arrows), and the reporter expression was markedly reduced by *441-GAL80* (Figure 6G, dashed arrows; Figure S6). The intersection between *441* and *918* thus confirmed their overlapping expression patterns and indicated that the neurons they label in common are necessary for aversion.

The ventromedial cell bodies and dorsal projection patterns are also characteristic of tyraminergic/octopaminergic neurons, which express tyrosine decarboxylase 2 (*dTdc2*) and can be targeted by *dTdc2-GAL4* [28] (Figure S6). We therefore combined *441-GAL4* and *dTdc2-GAL4* in the same fly and found that two *GAL4*s in combination labeled as many neurons in the posterior cluster as *dTdc2-GAL4* alone and slightly more than *441-GAL4* alone, confirming that the *441+tsh+* ventromedial neurons are also *dTdc2+* (Figure S6). *dTdc2* > *shi$^{ts1}$* did not affect aversion (Figure S6), which could either be caused by redundancy similar to the case of *EB* > *shi$^{ts1}$* or imply the involvement of other *441+918+* VNC neurons in aversion.

## Discussion

To our knowledge, this is the first direct demonstration that odorants modulate turn initiation and direction in freely walking insects. Moreover, aversive and attractive turns involve distinct kinematics. Intuitively, our quantitative analyses reveal that flies speed up and follow straighter trajectories after turning away from a noxious smell, which should shorten their exposure to potential harm. Such a strategy is not employed for attraction. Chemotaxis has been studied in tethered adult flies, paradigms in which mimicking the olfactory inputs a freely moving fly would encounter proved challenging. For example, in a "fly-on-the-ball" paradigm, aversion was not triggered, even using a strong repellent [4, 29]. In another study, flying flies responded symmetrically to aversive and attractive odorants [30]. Our more naturalistic approach provided new insights into the relationship between aversive and attractive chemotaxes.

In bacteria [1], aversion and attraction are achieved through bidirectional modulation of the same mechanism. Similarly, in *C. elegans*, aversion and attraction are thought to utilize a push-pull mechanism on one set of antagonizing command neurons [2]. Our genetic inactivation experiments suggest that, in flies, aversion is executed through specific neurons distinct from attraction. We identified two candidate circuit components, the EB and a subset of the VNC neurons, that appear redundantly necessary for aversive chemotaxis (Figure 6H). The EB is part of the central complex, defects in which are associated with uncoordinated walking [31]. In grasshoppers and cockroaches, activating central complex neurons induces specific kinematics [32, 33]. In the VNC, *dTdc2+* neurons are prominent candidates for mediating aversion, although other *441+918+* neurons might be involved. These neurons are homologous to dorsal or ventral unpaired median neurons in other insects because they are octopaminergic and show similar projection patterns [34]. The activity in these neurons is correlated with specific aspects of locomotion in locusts, crickets, and moths [34]. Given that *441* > *shi$^{ts1}$* flies display defects in aversive turn completion, but not initiation, we postulate that our genetic manipulation does not interfere with the perception, processing, decision-making, or even initiation steps of aversive chemotaxis but rather the execution of motor programs specifically necessary for this behavior. Our discoveries bridge the extensive investigation of olfactory processing in insects such as honeybees and moths [35] with studies focused on motor control mechanisms in species such as cockroaches and stick insects [36].

(E and F) Distribution of $\Delta\theta$ after turning, for events initiated when *441* > *shi$^{ts1}$* flies (E) were moving toward the odorant source (red dot in Figure 1C) during the control (n = 1,142) and aversive (n = 1,631) odorant periods. The modulation of direction is lost compared to *441-GAL4/+* (F) and *UAS-shi$^{ts1}$/+* (Figure 2C) controls.

(G and H) Angular speed peaks during illumination and then falls below baseline level in *441* > *ChR2* flies (G; n = 1,016 before illumination, n = 989 after illumination; n values are the same for speed), but not in control flies (H; n = 890 before illumination, n = 852 after illumination; n values are the same for speed).

(I and J) Speed increases after illumination in *441* > *ChR2* flies (I), but not in control flies (J). Gray bar represents the light-on period.

(A) and (B) show the same comparison as in the corresponding panels in Figures 1F and 1G. (C)–(F) show the same comparison as in the corresponding panels in Figures 2A–2D. (G)–(J) show Wilcoxon tests between the average angular speeds (G and H) or speeds (I and J) before (–0.2 s to –0.1 s) and after (0.4 s) illumination, with the light onset being time 0.

Please cite this article in press as: Gao et al., Specific Kinematics and Motor-Related Neurons for Aversive Chemotaxis in *Drosophila*, Current Biology (2013), http://dx.doi.org/10.1016/j.cub.2013.05.008



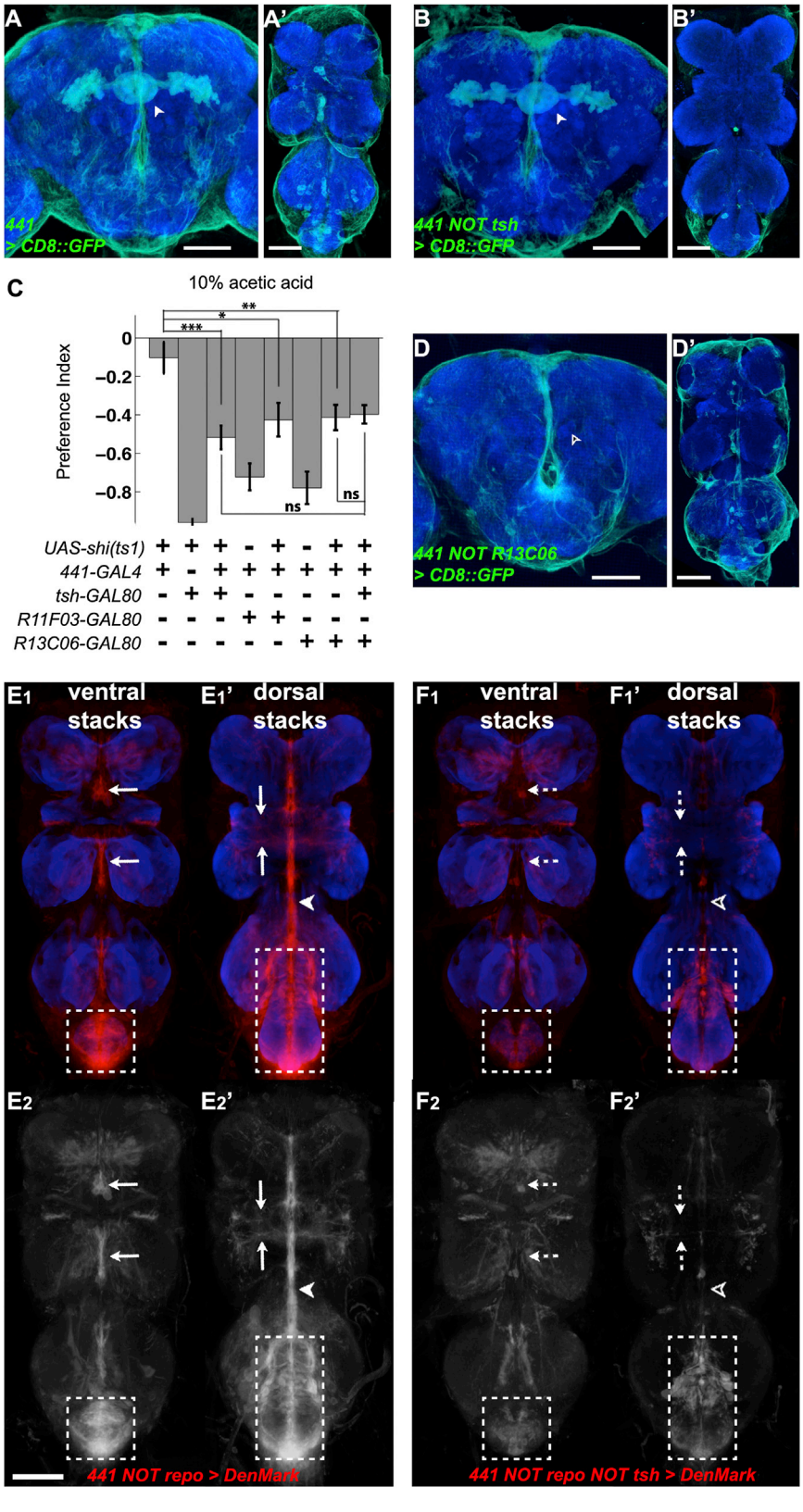


Figure 5. *441-GAL4* Targets Redundant Neurons Necessary for the Execution of Aversion

(A and A′) *441-GAL4* expression is visualized with a membrane-tagged *GFP* in the brain (A) and the VNC (A′). Arrowhead shows the ellipsoid body.

(B and B′) *tsh-GAL80* suppresses VNC expression of *441-GAL4*.

(C) Aversion in *441* > *shi$^{ts1}$* flies is partially restored with *tsh-GAL80* or *EB-GAL80*. The first column represents the same data as the last column in Figure 3B. Columns are mean PIs, and error bars represent SEM ($n \geq 4$); all tested pairs are labeled; t test was performed with Holm-Bonferroni post hoc correction.

(D and D′) *R13C06-GAL80* suppresses EB expression of *441-GAL4*, as indicated by the open arrowhead.

($E_1$–$F_2'$) Average *441-GAL4* expression without ($E_1$–$E_2'$) or with ($F_1$–$F_2'$) *tsh-GAL80* is visualized with a dendritic marker in the ventral ($E_1$, $E_2$, $F_1$, and $F_2$) and dorsal ($E_1'$, $E_2'$, $F_1'$, and $F_2'$) halves of the VNC after image registration against a standard VNC, shown with neuropil counterstaining of VNC ($E_1$, $E_1'$, $F_1$, and $F_1'$) or without ($E_2$, $E_2'$, $F_2$, and $F_2'$). Dashed boxes show abdominal ganglion; arrows show ventromedial cell bodies ($E_1$ and $E_2$; suppression indicated by dashed arrows in $F_1$ and $F_2$) and the corresponding dorsal-bilateral projections ($E_1'$ and $E_2'$; suppression indicated by dashed arrows in $F_1'$ and $F_2'$); arrowhead shows projection along the midline ($E_1'$ and $E_2'$; suppression indicated by open arrowhead in $F_1'$ and $F_2'$). Scale bars represent 50 μm.

motor pattern generation in adult flies has only been established for escape flight [26] and courtship song [22], both highly specialized for certain ethological functions. When a fly continuously explores the environment and updates its walking pattern, the division of labor between the brain and the VNC is less clear. Conceptually, one possibility is that circuit modules in the VNC only encode basic elements of locomotion. For example, right turns may always involve the same VNC circuit, and the only difference is their embedding within different sequences of actions based on the combination of descending signals from the brain. Alternatively, VNC circuit modules could be task specific; once a descending signal specifies the task, the details of the motor output will unfold according to a prewired VNC circuit. Our findings support the latter possibility in the context of aversive chemotaxis. In both vertebrates and invertebrates, artificial activation of neurons in the spinal cord or the VNC generates specific motor outputs, but rarely have these neurons been demonstrated to be necessary for specific sensory-driven tasks [36]. It would be interesting to test the generality of having autonomous motor-related circuits specifically responsive to certain sensory triggers.

It is intriguing that part of the aversion-specific circuit resides in the VNC and can be artificially activated to generate a pattern similar to aversive turns. Although the larval VNC is sufficient for substrate exploration [37], VNC autonomy in

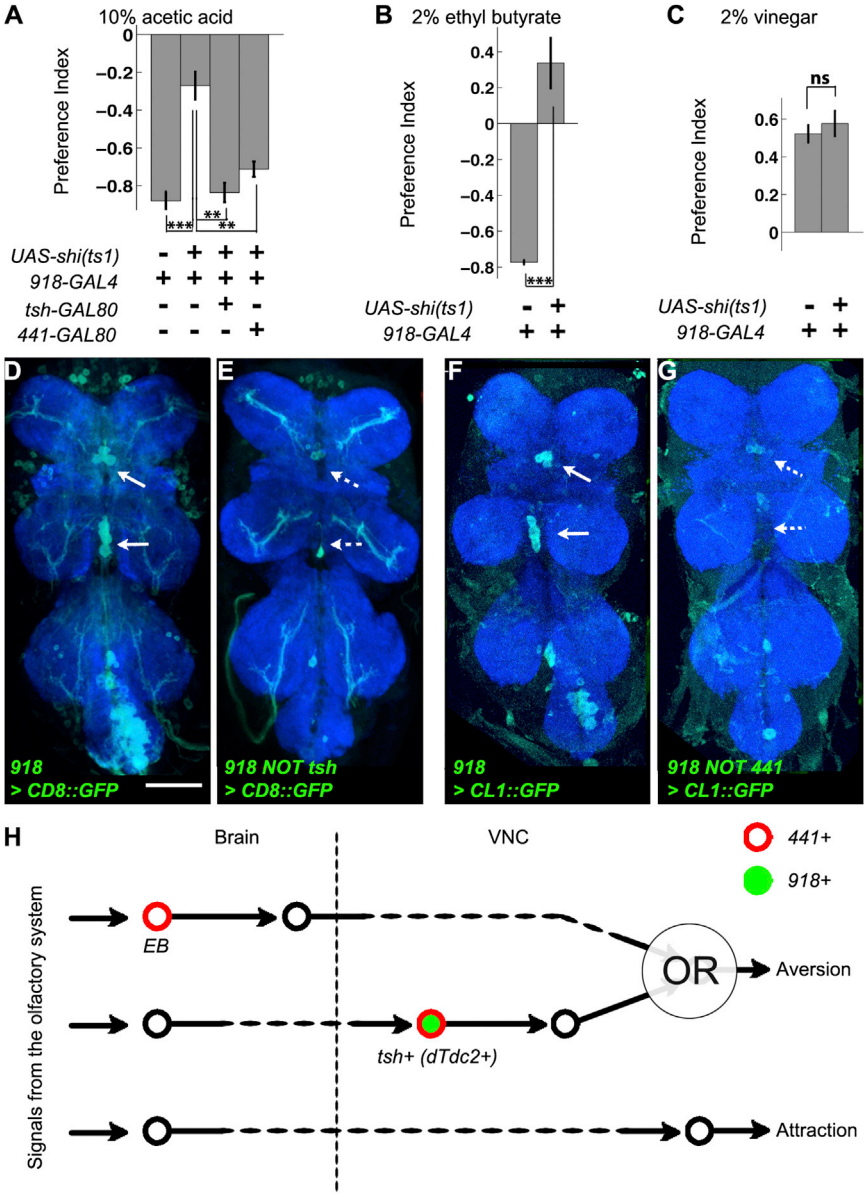


Figure 6. Analyses of *918-GAL4* Support the Role of Specific *441+tsh+* Neurons in Aversion

(A) *918* > *shi$^{ts1}$* attenuates aversion to 10% acetic acid, and this attenuation is suppressed by *tsh-GAL80* or *441-GAL80*.

(B) *918* > *shi$^{ts1}$* abolishes aversion to 2% ethyl butyrate.

(C) *918* > *shi$^{ts1}$* does not affect attraction to 2% vinegar.

Columns in (A–C) are mean PIs of multiple independent runs, and error bars represent SEM ($n \geq 3$); t test was performed with Holm-Bonferroni post hoc correction.

(D) *918-GAL4* expression in the VNC is visualized with a membrane-tagged *GFP*. Arrows point to the ventromedial cell bodies similar to those in Figures 5E$_1$–5E$_1'$.

(E) *tsh-GAL80* suppresses VNC expression of *918-GAL4*, including the ventromedial class, as indicated by the dashed arrows.

(F) *918-GAL4* expression is visualized with a destabilized *GFP*. Arrows point to the ventromedial cell bodies.

(G) *441-GAL80* suppressed the expression of *918-GAL4* in the ventromedial class, as indicated by the dashed arrows. Scale bars represent 50 μm.

(H) A schematic summary of the functionality of neuronal populations underlying aversive chemotaxis inferred from our genetic analysis. Each circle and the line attached to it represent a neuronal population and the direction of information flow; dashed lines represent potential intermediate layers of relay neurons. The "OR" logic gate near the end of the aversive circuit reflects the redundant roles of the pathways mediated by EB and *dTdc2+* VNC neurons.

Due to the asymmetry of the odorant contours, which curve toward the odorant source, a direct comparison between the frequencies of aversive and attractive turns was confounded by the difference in control frequencies (note that Figures 1F and 1G′ have a different y axis scale than Figures 1F′ and 1G). That is because a turn toward the odorant source does not constitute an attractive turn unless it is more curved than the local odorant contour.

For the temporal profiles of turns, speeds and angular speeds (in the arena-based coordinate system) were collected from 24 flanking frames (0.8 s) in each trajectory, aligned by the turning points, and averaged. For the analysis of turn initiation and direction, we partitioned each trajectory into forward walking and turning segments. Any data point with an angular speed above 400°/s was annotated as turning, and the rest were annotated as forward walking. The threshold was set based on the basal angular speed in Figures 1I and 1K. The angular speed was the absolute value of the orientation difference between two adjacent frames divided by the frame duration (1/30 s). The distribution was skewed such that the mean angular speed was near 400°/s, but the median was only 130°/s. But even for 400°/s, the orientation difference between two adjacent frames was just 400/30 = 13.3°. Thus, the apparently high baseline angular speed reflects the fact that the flies never follow truly straight trajectories. The first frame of one continuous turning segment was defined as its initiation, and the last frame was defined as its termination.

## Experimental Procedures

### Chemotaxis Paradigm

The four-quadrant behavioral arena was 16.5 cm × 16.5 cm and 1 cm deep [8]. It was placed inside a 33°C box in complete darkness. The airflow was filtered and saturated with water, entered each quadrant at a rate of 40 ml/min, and left through the central hole in the arena floor. One branch of airflow was controlled by solenoid valves through the LabVIEW software (National Instruments), so that for each trial air passed directly into one quadrant for 2.5 min and then was switched to bubble through 5 ml of water (for vinegar and acetic acid) or paraffin oil (for all the other odorants tested) containing an odorant with a specified concentration. The odorant source was replenished for each experiment.

### Behavioral Data Analysis

All analyses were performed with MATLAB (MathWorks). For aversion and attraction, all analyses were done with data from the time windows described in Figure S3. The only exception was learned aversion, where the first 2.5 min were analyzed to avoid memory extinction. Except for PI calculation, the data points within 0.5 cm of the arena walls were excluded to avoid the confounding effects of arena edges.

### Supplemental Information

Supplemental Information includes Supplemental Experimental Procedures, six figures, and six movies and can be found with this article online at http://dx.doi.org/10.1016/j.cub.2013.05.008.

**Acknowledgments**

We thank D. Luginbuhl and J. Brown for technical assistance; R.L. Davis, S.E.J. de Vries, G.S.X.E. Jefferis, M. Prakash, and T. Rohlfing for advice; B.D. Pfeiffer, A. Jenett, G.M. Rubin, and J. Simpson from the Janelia Farm for generously sharing unpublished reagents; Bloomington Drosophila Stock Center for flies; Addgene for plasmids; and C.J. Guenthner, W. Joo, T.J. Mosca, O. Riabinina, A. Ward, and B.C. Weissbourd for critiques. X.J.G. is supported by an Enlight Foundation Bio-X Interdisciplinary Fellowship. D.M.G. was supported by a Ruth L. Kirschstein National Research Service Award Postdoctoral Fellowship (F32EY020040) from the National Eye Institute. M.S. is supported by a postdoctoral fellowship from the Jane Coffin Childs Memorial Fund for Medical Research. C.J.P. was an associate and L.L. is an investigator of the Howard Hughes Medical Institute. This study was also supported by National Institutes of Health (NIH) grants R01-DC005982 (L.L.) and R01-EY022638 (T.R.C.) and an NIH Director's Pioneer Award, DP1 OD003530 (T.R.C.).

Received: February 16, 2013
Revised: April 14, 2013
Accepted: May 7, 2013
Published: June 13, 2013

**References**

1. Berg, H.C. (1975). Chemotaxis in bacteria. Annu. Rev. Biophys. Bioeng. *4*, 119–136.
2. Faumont, S., Lindsay, T.H., and Lockery, S.R. (2012). Neuronal microcircuits for decision making in C. elegans. Curr. Opin. Neurobiol. *22*, 580–591.
3. Louis, M., Huber, T., Benton, R., Sakmar, T.P., and Vosshall, L.B. (2008). Bilateral olfactory sensory input enhances chemotaxis behavior. Nat. Neurosci. *11*, 187–199.
4. Gaudry, Q., Hong, E.J., Kain, J., de Bivort, B.L., and Wilson, R.I. (2013). Asymmetric neurotransmitter release enables rapid odour lateralization in Drosophila. Nature *493*, 424–428.
5. Rajan, R., Clement, J.P., and Bhalla, U.S. (2006). Rats smell in stereo. Science *311*, 666–670.
6. Porter, J., Craven, B., Khan, R.M., Chang, S.J., Kang, I., Judkewitz, B., Volpe, J., Settles, G., and Sobel, N. (2007). Mechanisms of scent-tracking in humans. Nat. Neurosci. *10*, 27–29.
7. Bargmann, C.I. (2006). Comparative chemosensation from receptors to ecology. Nature *444*, 295–301.
8. Semmelhack, J.L., and Wang, J.W. (2009). Select Drosophila glomeruli mediate innate olfactory attraction and aversion. Nature *459*, 218–223.
9. Asahina, K., Louis, M., Piccinotti, S., and Vosshall, L.B. (2009). A circuit supporting concentration-invariant odor perception in Drosophila. J. Biol. *8*, 9.
10. Kreher, S.A., Mathew, D., Kim, J., and Carlson, J.R. (2008). Translation of sensory input into behavioral output via an olfactory system. Neuron *59*, 110–124.
11. Wang, Y., Chiang, A.-S., Xia, S., Kitamoto, T., Tully, T., and Zhong, Y. (2003). Blockade of neurotransmission in Drosophila mushroom bodies impairs odor attraction, but not repulsion. Curr. Biol. *13*, 1900–1904.
12. Suh, G.S., Wong, A.M., Hergarden, A.C., Wang, J.W., Simon, A.F., Benzer, S., Axel, R., and Anderson, D.J. (2004). A single population of olfactory sensory neurons mediates an innate avoidance behaviour in Drosophila. Nature *431*, 854–859.
13. Stensmyr, M.C., Dweck, H.K., Farhan, A., Ibba, I., Strutz, A., Mukunda, L., Linz, J., Grabe, V., Steck, K., Lavista-Llanos, S., et al. (2012). A conserved dedicated olfactory circuit for detecting harmful microbes in Drosophila. Cell *151*, 1345–1357.
14. Davis, R.L. (2004). Olfactory learning. Neuron *44*, 31–48.
15. Venken, K.J., Simpson, J.H., and Bellen, H.J. (2011). Genetic manipulation of genes and cells in the nervous system of the fruit fly. Neuron *72*, 202–230.
16. Katsov, A.Y., and Clandinin, T.R. (2008). Motion processing streams in Drosophila are behaviorally specialized. Neuron *59*, 322–335.
17. Branson, K., Robie, A.A., Bender, J., Perona, P., and Dickinson, M.H. (2009). High-throughput ethomics in large groups of Drosophila. Nat. Methods *6*, 451–457.
18. Gohl, D.M., Silies, M.A., Gao, X.J., Bhalerao, S., Luongo, F.J., Lin, C.-C., Potter, C.J., and Clandinin, T.R. (2011). A versatile in vivo system for directed dissection of gene expression patterns. Nat. Methods *8*, 231–237.
19. Kitamoto, T. (2001). Conditional modification of behavior in Drosophila by targeted expression of a temperature-sensitive shibire allele in defined neurons. J. Neurobiol. *47*, 81–92.
20. de Vries, S.E., and Clandinin, T.R. (2012). Loom-sensitive neurons link computation to action in the Drosophila visual system. Curr. Biol. *22*, 353–362.
21. Luan, H., Peabody, N.C., Vinson, C.R., and White, B.H. (2006). Refined spatial manipulation of neuronal function by combinatorial restriction of transgene expression. Neuron *52*, 425–436.
22. Clyne, J.D., and Miesenböck, G. (2008). Sex-specific control and tuning of the pattern generator for courtship song in Drosophila. Cell *133*, 354–363.
23. Joseph, R.M., Devineni, A.V., King, I.F., and Heberlein, U. (2009). Oviposition preference for and positional avoidance of acetic acid provide a model for competing behavioral drives in Drosophila. Proc. Natl. Acad. Sci. USA *106*, 11352–11357.
24. Pfeiffer, B.D., Jenett, A., Hammonds, A.S., Ngo, T.T., Misra, S., Murphy, C., Scully, A., Carlson, J.W., Wan, K.H., Laverty, T.R., et al. (2008). Tools for neuroanatomy and neurogenetics in Drosophila. Proc. Natl. Acad. Sci. USA *105*, 9715–9720.
25. Jenett, A., Rubin, G.M., Ngo, T.T., Shepherd, D., Murphy, C., Dionne, H., Pfeiffer, B.D., Cavallaro, A., Hall, D., Jeter, J., et al. (2012). A GAL4-driver line resource for Drosophila neurobiology. Cell Rep *2*, 991–1001.
26. Lima, S.Q., and Miesenböck, G. (2005). Remote control of behavior through genetically targeted photostimulation of neurons. Cell *121*, 141–152.
27. Jefferis, G.S., Potter, C.J., Chan, A.M., Marin, E.C., Rohlfing, T., Maurer, C.R., Jr., and Luo, L. (2007). Comprehensive maps of Drosophila higher olfactory centers: spatially segregated fruit and pheromone representation. Cell *128*, 1187–1203.
28. Cole, S.H., Carney, G.E., McClung, C.A., Willard, S.S., Taylor, B.J., and Hirsh, J. (2005). Two functional but noncomplementing Drosophila tyrosine decarboxylase genes: distinct roles for neural tyramine and octopamine in female fertility. J. Biol. Chem. *280*, 14948–14955.
29. Borst, A. (1983). Computation of Olfactory Signals in Drosophila-Melanogaster. J. Comp. Physiol. A *152*, 373–383.
30. Wasserman, S., Lu, P., Aptekar, J.W., and Frye, M.A. (2012). Flies dynamically anti-track, rather than ballistically escape, aversive odor during flight. J. Exp. Biol. *215*, 2833–2840.
31. Strauss, R. (2002). The central complex and the genetic dissection of locomotor behaviour. Curr. Opin. Neurobiol. *12*, 633–638.
32. Heinrich, R., Wenzel, B., and Elsner, N. (2001). Pharmacological brain stimulation releases elaborate stridulatory behaviour in gomphocerine grasshoppers–conclusions for the organization of the central nervous control. J. Comp. Physiol. A *187*, 155–169.
33. Bender, J.A., Pollack, A.J., and Ritzmann, R.E. (2010). Neural activity in the central complex of the insect brain is linked to locomotor changes. Curr. Biol. *20*, 921–926.
34. Braünig, P., and Pflüger, H.J. (2001). The unpaired median neurons of insects. Advances in Insect Physiology *28*, 185–266.
35. Martin, J.P., Beyerlein, A., Dacks, A.M., Reisenman, C.E., Riffell, J.A., Lei, H., and Hildebrand, J.G. (2011). The neurobiology of insect olfaction: sensory processing in a comparative context. Prog. Neurobiol. *95*, 427–447.
36. Pearson, K.G. (1993). Common principles of motor control in vertebrates and invertebrates. Annu. Rev. Neurosci. *16*, 265–297.
37. Berni, J., Pulver, S.R., Griffith, L.C., and Bate, M. (2012). Autonomous circuitry for substrate exploration in freely moving Drosophila larvae. Curr. Biol. *22*, 1861–1870.